Scientific report 96-03

KNMI

An acoustical array for subsonic signals

H.W. Haak

De Bilt, February 1996

KNMI Library
P.O. Box 201
3730 AE De Bilt
The Netherlands

Scientific report WR 96-03

De Bilt, 1996

Postbus 201
3730 AE De Bilt
The Netherlands

Telephone +31.30.220 69 11, telefax +31.30.221 04 07

UDC: 550.34.044.5
550.843
ISSN: 0169-1651
ISBN: 90-369-2107-4

© KNMI, De Bilt. Niets uit deze uitgave mag worden verveelvoudigd en/of openbaar gemaakt worden door middel van druk, fotocopie, microfilm, of op welke wijze dan ook, zonder voorafgaande schriftelijke toestemming van het KNMI.

KNMI

AN ACOUSTICAL ARRAY FOR SUBSONIC SIGNALS

by

H. W. Haak

ROYAL NETHERLANDS METEOROLOGICAL INSTITUTE, SECTION OF SEISMOLOGY

May 1991, February 1996

CONTENTS

AN ACOUSTICAL ARRAY FOR SUBSONIC SIGNALS

H. W. Haak

Royal Netherlands Meteorological Institute, Section of Seismology

Abstract

Array technique well known in seismology is applied to acoustical signals in the subsonic or infrasonic frequencyband. This is achieved by simply changing the detector, and scaling the dimensions of the array according to the differences between acoustic and seismic velocities. The design of a robust detector is taken from Hugo Benioff. The atmosphere is more homogeneous than the solid earth on length scales of the array but varies strongly with time due to wind and temperature variations. This leads us to reevaluate the array design. Recent techniques to process the data, borrowed from seismology, are described. Finally various trade-off's in array processing are mentioned in order to make clear that different objectives could guide between various array processing techniques. Some results are discussed from measurements with a six-element array mainly focussed at sonic boom detections.

Introduction

The application of array techniques is well established in seismology. The measurement of coherent seismic waves by means of a collection of separate detectors, each having equal properties, yields valuable information such as horizontal wave velocity, azimuth of the incoming wave and dispersion properties. These are virtually all the parameters of a given plane-wave field in space and time. By summing the individual time series of the detectors with appropriate time delays, some noise reduction can be achieved. Usually this reduction in noise is of the order of $\sqrt{N}$, where N is the number of sensors. In the field of acoustics the concept of an array of detectors seems to be less common than in seismology. Although in the nineteen-sixties arrays of microbarographs were employed to detect pressure waves from atmospheric nuclear explosions: Large Aperture Microbarograph Array (LAMA). For the same reason today the interest is growing in the context of monitoring a comprehensive nuclear testban.

In the late sixties a number of detectors were developed also with the purpose to detect nuclear explosions: low frequency microphones, the Daniels Pipe arrays (Cook, 1971), microbarographs etc. One of the detectors which we employed in this study dates from before this period. It was constructed by Hugo Benioff in 1939. The detector consists of a low frequency loudspeaker mounted in a closed airtight volume, and it is operated as a pressure detector. The response is flat to pressure change. Surprisingly another low frequency detector is available that is both very small and low budget: an electret microphone. This response is flat to pressure.

Current developments both in computers and in mechanical technology make that today highly efficient and low cost acoustic arrays are possible. Also when equipped with more sophisticated pressure sensors such as very low frequency quarts crystal pressure sensors.

Not only the ideas on the instrumentation adapted were from seismology. Also, the motivation of this study had a seismological background. In the northern part of the Netherlands up till 1991 seven earthquakes occurred that are induced by natural gas extraction. Besides these well-recorded events we received numerous reports of rumblings and vibrations. Sometimes these reports were covering an area of over 10.000 km^2, sometimes only reports were given from a very limited area. From analysis of the Netherlands network of seismographs it followed that these events were all of atmospheric origin; low frequency sound waves in the seismic frequency band.

Further analysis of these signals seems appropriate. The occurrence of other historic mysterious sounds strengthen us to investigate these findings. From 1900 onwards people along the coast of the Netherlands experienced the so-called "zeepoeffers" most often in the summer with calm weather conditions. These brontides (from the Italian brontidi), as these sounds are called in the Anglo-saksian literature (Gold and Soter, 1979) are often observed in coastal regions without being explained by a common physical phenomenon. To our surprise the signals in the low audible and infrasonic frequency range provided a model example of the application of array techniques.

Instrumentation

The instrumentation of the acoustical array we designed consists of a set of six acoustical detectors and the central data acquisition computer including amplifiers, anti-alias filters and a time-keeping system. We accomplished the off-line analysis with a separate personal computer. Data transfer between the data-acquisition PC and the off-line analysis PC was done via floppy disks or via a local area network. For remote sites we used dialup telephone lines with the PC-Anywhere program, between PC's we used the Lantastic filetransfer program. Finally the data is stored on an optical disk. In figure 1 an overview is given of the whole system.

The acoustic detector

The design of the low frequency microphone we choose is dating from 1939 (Benioff, 1939). B. Gutenberg used this kind of loudspeaker-microphone to probe the velocity structure of the atmosphere (Gutenberg, 1939). It consists of a low frequency loudspeaker (woofer) mounted in a box, just like a pressure box in audio technique. When the atmospheric pressure outside the box is changing, the cone of the speaker will move like a piston. The magnet-coil assembly will generate a voltage proportional to the velocity of the cone. Usually a small leak is introduced to equalize the pressures over long time periods, such as from temperature variations and changing ambient atmosphere pressure. The movement of the cone ΔX upon a pressure variation ΔP is given by:

$$\Delta X = \Delta P \frac{-A}{A^2 \gamma P / V + C_c} \tag{1}$$

In which A is the area of the cone, P is the ambient atmospheric pressure, V is the enclosed volume of the box, γ is the ratio of heat capacities at constant pressure and constant temperature. C_c is the force constant of the elastic hinges of the cone itself. This force constant can be calculated from the resonance frequency f_{res} of the unmounted speaker:

$$f_{res} = \frac{1}{2\pi} \sqrt{\frac{C_c}{m_c}} \tag{2}$$

The mass of the cone is m_c. The output voltage V_{out} of the detector is proportional to the velocity of the cone:

$$V_{out} = K \frac{d(\Delta X)}{dt} \tag{3}$$

K is the generator constant of the magnet-coil combination. The output voltage is a measure of the pressure change. From equation (1) it becomes clear that if a speaker with a very low resonance frequency is used, so C_c is small compared to $A^2 \gamma P/V$, the system sensitivity is given by:

$$\frac{\Delta X}{\Delta P} = \frac{-V}{A \gamma P} \tag{4}$$

So one can optimize the output by enlarging the enclosed volume V while keeping a small diameter of the loudspeaker. This the case of a true piston. When the opposite is true, C_c is large compared to $A^2 \gamma P/V$ then the systems sensitivity is given by:

$$\frac{\Delta X}{\Delta P} = -\frac{A}{C_c} \tag{5}$$

In this case a larger area of the speaker will increase the sensitivity. This is the case of a pure elastic bellows. The trade-off between V, C_c and A can be found by differentiating equation (1) with respect to A, in order to maximize the sensitivity:

$$A = \sqrt{\frac{C_c V}{\gamma P}} \tag{6}$$

Most of the above formulas also apply to microphones with elastic membranes or bellows. With slight modifications the same holds when feedback is applied. In that case the membrane is driven back to the equilibrium position with an external force that balances the external pressure. This stiffens the elastic system and enlarging C_c. Feedback transfers the dynamics of the system from the mechanical parts to the electronics, where it is easier to handle.

When the detectors are placed in the open field several factors are important to ensure stable operation with respect to wind and weather. Figure 2 shows most of the precaution measures. The system is placed upside down to avoid rain coming in. In order to avoid large pressure variation due to wind the detector is placed close to the ground on a lawn and Dacron wool (fibre fill) is used. After one year of operation we found that this material was disappearing in spring because it was considered most useful by birds.

The detectors we used had a volume of 30 litre and were equipped with the Philips speaker AD10202/W8. The choice of this speaker was mainly motivated by the availability of accurate data sheets: notably the parameters K, A, C_e and f_{res}. We noticed that with very low ambient temperatures (-20 °C) the elastic rubber ring around the stiff cone lost its elastic properties. In this case the output levels were reduced.

The dynamical response of the detector is given in figure 3. Clearly there are 3 regimes, the low frequency regime: the small leak is levelling out the long period pressure differences. The time constant of the leak determines the corner frequency. The middle frequency range is the working range of the detector. The high frequency range, beyond the resonance frequency of the speaker is a second order roll-off towards higher frequencies. Considering the dynamic response of the detector, it is efficient to choose the resonance frequency of the mounted loudspeaker close to the Nyquist frequency of the data-acquisition system or the corner frequency of the anti-alias filter.

Besides the 30-litre detector we experimented with a 5-litre version. The much smaller detector (30 x 15 cm) works equally well provided a low noise preamplifier to compensate for the ten times lower output voltage. The speaker we used was a woofer from a car stereo system with smaller dimensions (VISATON WS 13 NG, 8 Ohm). Still smaller dimensions are possible. One of the advantages of this kind of detector is its inherent low-price and easy construction. Some care should be taken to ensure that the controlled leak is not bypassed by the possible leak of the porous material of the cone of the speaker.

The electret-detector

Quite by accident we discovered that cheap and small electret microphones have reasonable flat responses down to 1 Hz. In comparison with the loudspeaker detector the electret microphone is generally more sensitive towards lower frequencies. Within a given set of electret microphones a slight variation occurs of the low-frequency response and output level, therefore we selected approximate equal individuals from a larger set. We operated acoustic arrays with both (woofer and electret) detector types. When infrasonic waves are measured with this microphone, the highest noise amplitudes are due to wind induced pressure variations. Therefore, considerable care should be taken to suppress this noise.

Noise reducing structures

We used spatial filtering to reduce the noise signals, since we wanted to keep the flat frequency response. Acoustic signals are not attenuated considerably when integrated over areas smaller than half their wavelength. In general, due to the temperature profile as a function of height the acoustic waves propagate almost in a horizontal direction over the array. This is a marked difference with seismic wave propagation. The acoustic wavelength corresponds rigidly to a certain frequency, only depending on the velocity of sound. Due to the turbulent character of wind field, pressure variations at a certain frequency correspond on average to a variety of wavelengths. Therefore, one can use spatial filtering such as spatial integration to discriminate between acoustic and wind signals.

Daniels (Cook 1971) solved this problem earlier for very low frequencies by using large circular pipe arrays. We designed a sensor in the frequency range from 1 Hz to 50 Hz by scaling down the circular pipe. A porous garden hose (Gardena) works equally well. The electret microphone is mounted inside a thick walled (3.5 mm) plastic tube. The outside diameter is 32 mm. The 8-metre tube is bend into a closed circular shape with a diameter of 2.5 metres. The outside pressure is measured by the microphone through twenty equidistant holes 0.8 mm in diameter.

The acoustic resistance of the holes is far higher than the resistance of the tube itself. Therefore, the pressure inside the tube is the spatial average of the ring's circumference. The whole ring is buried below 5 to 10 cm course gravel, to avoid direct impact of the wind. In comparison with a single point detector a tenfold reduction of wind noise was achieved with the ring-detector. See figure 4. Another possibility is a noise reducing structure that has radial tubes. In the centre of the "spider" the detector is situated. The spacing of the small holes can than be subject to optimalisation. When the number of radial tubes exceeds six, the circular tube is more material efficient.

A still somewhat an unsolved problem is the accumulation of moist. We have tested various solutions none with satisfactory results. The best solution is probable to heat the sensor at temperatures slightly above the ambient temperature. The problem is most pronounced with the electret microphones. Another problem arrises when small particles and dirt are clogging the small holes in the noise reducing pipe. These practical issues require further research.

The data-acquisition system

The PC-based data-acquisition system was built with standard boards. With the 16 channel amplifiers and multiplexer board, the six acoustic detectors were recorded with two different gains. Also, a separate time channel was included consisting of a DCF77 radio clock. This clock made an absolute time calibration possible. We used a 12-bit A/D converter of the type DT 2824 or 2821 of Data Translation. We also used a 16-bit A/D converter of the type PCL-816/814B of PC-LabCard from Advantech Co., Ltd. with an adjusted data-acquisition program. The sampling frequency was set at 120 Hz. The backbone of the data-acquisition system was software from the IASPEI Toolbox, Volume I (Lee, 1989). This software is in standard use by many seismological stations. We altered the program to accommodate the 16-bit A/D converter, to incorporate filtering procedures and to list a number of auxiliary parameters on-line, such as the temperature.

A critical part of the software is the event detector. On each channel a long term average over short term average trigger (LTA/STA) is run. Only when five out of six channels are triggered an event is declared and the data is stored on disk. This double event trigger works quite well. Even in stormy weather the number of false events stayed within acceptable numbers. However, it may take some time to adjust the parameters of the LTA/STA detector. We intend to install just like our seismic systems a large (1 Gbyte) harddisc in the data acquisition PC's. Such a data storage device is a large ringbuffer. In this way we are less dependent on the trigger algorithm.

The acoustic array

A collection of separate detectors with similar properties is called an array. The detectors of an array sample signals in the spatial domain. The coherent signals from the detectors are supposed to originate from plane waves in most cases. Sampling in the time domain is usually accomplished with equidistant sample time intervals. Since in the spatial domain each sample is the equivalent of a detector there is the need for a much more efficient design of an array.

With an array one measures essentially the spatial form of the incoming waves. After the Fourier transforms involving space and time one obtains the frequency-wavenumber spectrum. Consequently the phase velocity in the horizontal plane at each wavelength or frequency of the wave train is known. When also the temperature is measured the phase velocity of the wave train is known.

In many problems the velocity of plane waves is not the most practical unit, since the physical plane wave quantities involved propagate with a functional dependence on space and time via:

$$(t - \frac{\hat{l} \cdot \vec{r}}{c}) = (t - \vec{p} \cdot \vec{r}) \qquad (7)$$

The unitvector $\hat{l}$ is the direction of propagation the normal of the wave front, t and $\vec{r}$ are the time and spatial coordinates respectively, and c is the wave propagation velocity or phase velocity.

The vector:

$$\vec{p} = \frac{\hat{l}}{c} \tag{8}$$

is called slowness vector. The slowness, e.g. the reciprocal of the apparent velocity in a certain direction with unit direction vector $\hat{n}$ is given by the product $\vec{p} \cdot \hat{n}$. Since most arrays are situated on the earth's surface, the horizontal component of slowness is measured.

The relation between horizontal wavenumber $\vec{k}_h$, horizontal slowness $\vec{p}_h$ and frequency ω is given by:

$$\vec{k}_h = \omega \vec{p}_h \tag{9}$$

For sound waves with very low dispersion it is most handy to produce plots of the power P as a function of the slownesses p_x and p_y instead of the wavenumbers k_x and k_y. This is called a the slowness plot. An easy, but not necessarily the best way to produce such plots is via the expression for the computation of frequency-slowness spectra:

$$P(\omega, \vec{p}_h) = \left| \sum_{n=1}^{N} S_n(\omega) e^{i\omega \vec{p}_h \cdot \vec{r}_n} \right|^2 \tag{10}$$

The complex Fourier spectrum of the n^{th} detector is $S_n(\omega)$, $\vec{r}_n$ is the position vector of the n^{th} detector. N is the total number of detectors. This calculation is usually followed by an integration over a certain frequencyband ω_1, ω_2:

$$P(\vec{p}_h)_{\omega_1, \omega_2} = \int_{\omega_1}^{\omega_2} P(\omega, \vec{p}_h)\, d\omega \tag{11}$$

The integration over the frequencyband can in principle be omitted when narrow band signals of known frequency are considered. With broadband signals however, this integration is very effective to lower unwanted peaks in the power plot P. The main lobe is then more easy to identify.

Array design

Since a finite number of spatial sampling points produce a distortion in the measured two-dimensional wavenumber or slowness spectra, it is of prime importance to optimize the array design. The distortion arises because the measured spectrum is a convolution of the true spectrum with the array response function. The array response function is given by:

$$R(\omega,\vec{p}) = \frac{1}{N}\sum_{n=1}^{N} e^{i\omega\vec{p}\cdot\vec{r}_n} \qquad (12)$$

Usually plots are presented of RR^* or $|R|$ as a function of p_x and p_y for a specific frequency ω, sometimes the power is given in dB, so a logarithmic scale is used.

In the following discussion on array design we give the arguments given by Haubrich (Haubrich, 1968). In general we want to optimize the array response with respect to three features:

a. the resolution of the main central lobe (large resolution),
b. the distance between the central lobe and the other (alias) main lobes (large Nyquist wavenumber, bandwidth),
c. the amplitude ratio between the central lobe and the secondary lobes, e.g. between the central lobe and (alias) main lobes (low ripple between main lobes, errors).

To reach a trade-off between these conflicting demands on the array response we have three distinct categories of parameters available to obtain optimal power spectra. It should be noted however that "optimal" usually strongly depends of the specific problem at hand. The categories are:

a. the N coordinates $\vec{r}_n$ of the detector sites,
b. the weights applied as a tapering function either as a function of the relative position of the detectors or as a function of the various detector separation distances,
c. the specific method of array processing techniques, subsequent data analysis and power spectrum estimation, e.g. high resolution methods, the use of a cleaning procedure etc.

This problem of optimalization cannot be solved with general methods. However, a reasonable way to approach this problem is first to find a convenient array lay out (a) by trial and error methods. Then solve analytically the weight problem (b). The subsequent choice of an array processing technique (c) depends usually strongly on the specific boundary conditions for the problem at hand. When classical methods (low resolution) are chosen the demands on the resolution are normally solved through the choice of the number of array elements and the array lay out.

It is noted however, that to optimize an array the N time series themselves should be explicit part of the procedure and not just a simple one frequency sinusoidal signal. This opens the possibility for efficient correlation techniques and is a way around to strict wavenumber bounds. In general larger arrays are possible without aliassing problems. It is also noted that the array response is known with precision. It is therefore possible to deconvolute the measured f-k spectra.

If we work out the expression RR^* for the array response and introduce a weight function w_{js}, we obtain the expression:

$$RR^* = \sum_{j=1}^{N} \sum_{s=1}^{N} w_{js}\, e^{i\omega\vec{p}(\vec{r}_j - \vec{r}_s)} \tag{13}$$

This expression follows also when the power spectrum is estimated from the Fourier transform of the cross-correlation (Smart, 1971).

The array with the sample points r_j has an associated set of points defined by:

$$\vec{D}_m = \vec{r}_j - \vec{r}_s \tag{14}$$

This set is called the coarray, it consists of N^2 points of which N are zero. From the definition is it clear that the points $\vec{D}_m$ occur in pairs: $\vec{r}_j - \vec{r}_s$, $\vec{r}_s - \vec{r}_j$.

There are at most $\hat{M} = N(N-1)/2$ pairs. In symmetrical arrays some $\vec{r}_i - \vec{r}_j$ values produce the same points in the coarray. We call the number of independent pairs of points of the coarray M. With this, the expression (13) can be rewritten as:

$$RR^* = w_0 + 2\sum_{m=1}^{M} w_m \cos(\omega \vec{p} \cdot \vec{D}_m) \tag{15}$$

Equation (15) gives insight in the design rule that the quality of the array, given by a combination of resolution, bandwidth and errors, increases when the number of independent points M in the coarray increases.

Equation (15) can be interpreted as a Fourier series to obtain a desired response RR^*. When more terms are included a more accurate fit of the desired response is obtained. If various points in the summation over M coincide it will change the weight factors for each frequency accordingly.

The above arguments make also clear that apart from the number of sinusoids M also the two-dimensional distribution of coarray points is of importance. In general a homogeneous distribution of coarray points within a circle with radius R_c will yield a response with a satisfactory trade-off between resolution band width and ripple.

The resolution is Δp related to the radius R_c through the approximated expression:

$$\Delta p \approx \frac{1}{R_c} \tag{16}$$

The bandwidth in terms of the Nyquist wavenumber or slowness p_N is given by:

$$p_N \approx \frac{1}{r_c} \tag{17}$$

in which r_c is the average distance between the coarray points. All of this is well known in standard time series analyses. The ripple is a complicated function of the homogeneity of the

distribution of coarray points. If we disregard the weights w_m for the moment then it is clear from the above arguments how we should design the coarray, i.e. as a homogeneous set of points within a certain radius.

Focussing on the symmetry of the coarray only two types of symmetric patterns can be used: a square pattern and a hexagonal pattern. Square coarray patterns suffer in general from the fact that for small N the number of independent pairs of points M in the coarray will be less than $\hat{M}$, or a number of points of the coarray will be outside the circle. Hexagonal coarray patterns are easy to construct from array patterns with a three fold symmetry. This class of arrays is called isometric (Haubrich, 1968). Clearly this type of symmetry is most efficient for small N, because of the combination of the plane filling property of hexagonal symmetry and the fact that threefold symmetry will lead to sixfold symmetry in the coarray.

Quite another class of arrays is possible, derived from circular symmetry especially assemblies of uneven numbered polygons are used. The seismic array of Hagfors and the NORESS type arrays are recent examples of polygon arrays. In this type of design the alignment of one ring to the other is more or less arbitrary.

Haubrich distinguishes for linear and two-dimensional arrays between an "optimal" array and a "perfect" array. A perfect array is defined as an array for which $M = \hat{M}$ and the coarray is uniform. This means for a linear array that the coarray consists of pairs of equidistant points at: $\pm 1, \pm 2, \pm 3, \ldots \pm n$. When M is as large as possible, the array is called optimal. With slight modifications the same definitions can also be applied to the two-dimensional case. The number of perfect linear arrays is limited to $N \leq 4$. In the same sense the largest perfect two-dimensional isometric array can be constructed for $N = 6$.

We choose this six-element array configuration for our acoustic array illustrated in figure 5a. The coarray is given in figure 5b. The perfect or optimal response however discards the use of weights, or the use of other than classical methods. On the other hand the perfect or optimal arrays are not trivial solutions to the problem.

Operating modes with arrays

The above arguments will lead to an array configuration. Once installed in the field the next step is to operate the array in the best way, considering the type of data and the aim for specific results. In our case, with the perfect six element isometric array, the detector separation was 25 metres. Considering the lowest signal velocity of ca. 300 m/s and a Nyquist wavelength (λ_N) of ca. 50 m. we can handle frequencies up to 6 Hz. In practice however this is a far too strict frequency limitation.

The construction of an analog spatial anti-alias filter is not easy. In most cases this problem is solved in the time domain by choosing a Nyquist frequency in such a way that given a known dispersion relation wavelengths shorter than λ_N are filtered out in the time series of each detector.

Operating the array above the Nyquist wavenumber is possible because of a priori knowledge of the signal in the time domain. For instance we know that the maximum slowness is ca. 3.3 s/km for sound waves. Secondly, a lot of signals like sonic booms have a broad frequency/wavelength content. Especially the broad frequency/wavelength content of signals make it possible to operate the array at least a factor 5 above the Nyquist wavenumber, the Nyquist frequency was 60 Hz. The background of this paradox lies in the integration over a frequency band by which the lower frequency guide the higher ones. In figure 5e the array response is given over a broad frequency range. This figure shows the increased resolution and the fact that the true main lobe in slowness space is undistorted while the alias lobes are smeared out. In the figures 5c and 5d the array responses are given at 10 Hz.

Given these facts on resolution enhancement with broadband signals, one can relax somewhat on the resolution of the true-main lobe and gaining less ripple by applying a taper function on the array for instance, with a two-dimensional Hamming taper. See figure 5d. In the case of the 6-element array the ripple is 13% of the main lobe in the untapered case and 3% in the tapered case a factor of 4, at the expense of a 20% decrease in resolution. The choice of the tapering function can be optimised through the Backus-Gilbert algorithm which treats the trade-off between errors and resolution in a more formal sense (Backus, 1968).

An alternative way to remove the ripple and the side lobes altogether can be achieved with the procedure CLEAN, originally developed in radio-astronomy by Högbom (Högbom, 1974) and later introduced in seismology by Nolet and Panza (1976). This procedure proceeds in five steps as follows:

a. Find the maximum of the plot at p_x, p_y.
b. Subtract from the normalized P-plot a certain fraction of the theoretical array response.
c. Store the coordinates of the maximum p_x, p_y and the fraction.
d. Proceed to point a, if the residual P-plot contains power exceeding a certain limit else,
e. Sum back over all the obtained p_x and p_y values from stage c with a new response of a hypothetical array with one main lobe only.

Normalization

When working out the f-k spectra or ω-p-plots some care should be taken with regard to proper normalization of the Fourier spectra of each detector, e.g. the functions $S_n(\omega)$. There are three possibilities:

a. No normalization at all. In this procedure the differences in the amplitude factors will enter the summation as weight factors when the magnification of the detectors is not set exactly equal, thereby lowering the resolution.
b. Normalization of $S_n(\omega)$ with $|S_n(\omega)|$. This normalization will remove differences in amplitude response, leaving only differences in the phase response. In analysing broadband data with strong frequency dependence within the band, the danger exists that low amplitude frequencies are dominating the P-plot.
c. To avoid at least in an average sense both above situations, a third normalization scheme is used. It uses the amplitude terms averaged over all detectors.

None of those normalization schemes seems to be ideal, but we tend to favour the third scheme, given reasonable tolerances on amplitudes of the individual detectors to start with. This can be checked by comparing scheme a and c. In narrowband applications scheme b seems appropriate.

Delay and sum method calculation of the best beam

Once the horizontal slowness vector is known, both the horizontal propagation speed and the azimuth of the signal are known. From this the time delay $\Delta\tau_j$ at each detector can be calculated using:

$$\Delta\tau_j = -\vec{p}\cdot\vec{r}_j \tag{18}$$

So through shifting each trace with the calculated delay to align the individual traces, and then sum or weight and sum the traces, a so-called "best beam" can be calculated. Since the signal is known only at the time intervals of the sampling frequency this delay and sum procedure is done in the frequency domain and not in the time domain. The result: the best beam, gives the best estimate of the signal with noise reduction of a factor of the order of $\sqrt{N}$ where N is the number of detectors. Within the same procedure we calculate the integral of the signal, because the output of some detector types represents differentiated pressure. Best beam methods can also be employed in real time event detection (Smart, 1971).

Correlation method

Well known alternatives for the method of f-k analysis as well as for event detection are correlation techniques (Cansi, 1993), (Grachev, 1978). The basic formula for cross-correlation is given by:

$$c_{g,h}(\tau) = \int_{-\infty}^{\infty} g(t)\,h(t-\tau)\,dt \;\;;\;\; c_{g,h}(\tau) = c_{h,g}(-\tau) \tag{19}$$

The functions *g(t)* and *h(t)* are the time series of two array elements. The time lag τ measures the relative shift of the two channels. The time lag of the absolute maximum of the function $c_{gh}(\tau)$ corresponds to the time delay τ_{gh} between the signals in the channels g and h. In some cases the maximum of the correlation function is not quite clear due to the oscillatory motion of the signal or noise components. Other maxima can occur at the characteristic period of oscillation in the case of narrow band signals. A large ambient noise makes proper identification of the maxima difficult. This ambiguity is the correlation counterpart of the Nyquist-problem. The fast way to calculate the correlation function is by the Fast Fourier

Transform (FFT):

$$C_{g,h}(\omega) = FT(c_{g,h}(\tau)) = G(\omega)\,H^{*}(\omega) = A(\omega)\,e^{i\phi_c(\omega)} \tag{20}$$

The phase function $\phi_c(\omega)$ can be interpreted in two equal justified ways. First it can be interpreted as a phase shift in the space-domain. Then it follows that $\phi_c(\omega) = \vec{k}_h \cdot \vec{r}_{gh}$ (Grachev, 1978). This leads to standard f-k analysis. Second $\phi_c(\omega)$ can be interpreted in the time-domain as $\phi_c(\omega) = \omega\tau_{gh}$. This leads to the correlation method (Cansi, 1993). The two methods are connected through the dispersion relation $c = \omega/|k|$. So the methods are in principle fully equivalent. The differences can be found in the ease of calculation and the way intermediate steps can be used to build in to ensure right results. For example, the intermediate rule that $\Sigma\,\phi_c(\omega) = 0$. This rule is equivalent with the Chasles equations with respect to time delays. Another intermediate calculation can based on the fact that an auto-correlation is symmetric with respect to time lag and has only one maximum when broadband signals are considered.

The time delays τ_{gh} are calculated from the slope of the phase as a function of frequency:

$$\tan(\phi_c(\omega)) = \frac{Im(C_{g,h}(\omega))}{Re(C_{g,h}(\omega))} \qquad \tau_{gh} = \frac{d\phi_c}{d\omega} \tag{21}$$

Just like the calculation of the group delay in standard time series analysis. The slope of the phase function can be determined by a weighted least-squares fit, after a course estimate of the delay time to avoid the 2π ambiguity. The weighting function can be the coherency function:

$$|\Gamma_{g,h}(\omega)| = \frac{|G(\omega)\,H^{*}(\omega)|}{(|G(\omega)G^{*}(\omega)|\;|H(\omega)H^{*}(\omega)|)^{1/2}} \tag{22}$$

So with the correlation function the time differences of the signals between all the *N(N-1)/2* combinations of array elements can be calculated. The consistency can be checked with the Chasles relation in order to avoid any ambiguity due to narrow band signals:

$$\tau_{ij} + \tau_{jk} + \tau_{ki} = 0 \tag{23}$$

In some cases a much more simple determination of the time lags is more appropriate, for instance by just determining the maxima of the correlation functions. The expected duration of the signals and the array layout will determine the time window of the time series to be correlated and the maximum time lag respectively for non-moving sources.

When all the delay times are known a fit of the time delays can be made to slowness and azimuth or to other relevant parameters such as the curvature of the wave front. In this analysis non-planar waves are allowed. The correlation method uses the complete frequency band of the signal, but it is not well suited to handle multiple signals.

A natural extension of the correlation method is to calculate, instead of the two-function cross-correlation, a multidimensional cross-correlation function:

$$sc_{g,h,i,j,\ldots}(\tau_1,\tau_2,\tau_3,\ldots) = \int_{-\infty}^{\infty} g(t)\, h(t-\tau_1)\, i(t-\tau_2)\, j(t-\tau_3)\ldots dt \qquad (24)$$

This super-correlation function has in principle *N-1* independent time delays. Therefore in order to limit this number various assumptions can be used to obtain results. When for instance a plane wave is assumed, given the array configuration, the time delays can be calculated given slowness and azimuth or the horizontal wave numbers and the velocity of wave propagation.

Another extention of the method can be found in the fact that the cross-correlations in this application are symmetric around the time lag between the signals of pairs of array elements since the cross-correlations here are essentially auto-correlations of shifted signals burried in noise.

With correlation methods it is easy to transform the incoming channels of an array into time series of signal amplitude, azimuth, horizontal slowness or velocity and the inclination of the signal when the ambient temperature is measured (Baumeler, 1991). This approach is useful for identifying the sources of the infrasonic disturbances with only one array.

The optimal array configuration for the correlation method can differ from an array that is operated with f-k analysis, because in the correlation method more subtle step by step approach can be followed in which checks can be build in every step. This could lead to a less sophisticated array design such as a simple square array layout. In a symmetrical 4-station square array with large distances between array elements in principle one element is redundant. When one element fails, the remaining configurations are all equal. Large distances between array elements can be chosen in accordance with the coherence length of the acoustic signals since spatial aliasing is removed in this method. The conclusion that an array can be larger when broadband signals are considered, then an array design on the basis of the centre band frequency only, can also be drawn in f-k analysis.

Noise considerations

When signals with low amplitudes are detected, noise considerations become important. Usually one makes a distinction between the noise of the detection system itself and noise outside the system. The latter can be qualified as a continuous background of unwanted signals; atmospheric pressure noise. In a well-designed system the systems noise should be well below the atmospheric pressure noise. With the current technical means this is easy to achieve.

To measure the noise characteristics we performed a number of separate experiments.
By placing two sensors as close as possible together the additive system noise was measured for the two or more collocated sensors. By putting the sensors in a line with various distances between the sensors we could measure the atmospheric noise coherency. The output of the j^{th} channel, $s_j(t)$ can be defined as the sum of the signal input $u_j(t)$ and $n_j(t)$ the systems own measurement noise. $u_j(t)$ can be a true signal as well as pressure noise. So:

$$s_j(t) = u_j(t) + n_j(t) \tag{25}$$

When two or more sensors are collocated then $u_j(t) = u_k(t)$. The input signals are the same, and the systems noise is uncorrelated:

$$\langle n_j(t) \cdot n_k(t) \rangle = \delta_{jk} \tag{26}$$

The inner product of x and y is denoted as $\langle x \cdot y \rangle$, δ_{jk} is the Kronecker delta function (Batties, 1989).

With these correlation functions we can separate the atmospheric pressure noise from the systems noise, leading to a signal to noise ratio. There is however a much simpler method for obtaining virtually the same results. Plotting the individual samples of the two time series $s_j(t)$ and $s_k(t)$ as x and y coordinates one obtains a pixel plot. This is illustrated in figure 6. For the two collocated sensors the two statistical noise distributions are clearly visible; the broad distribution of the coherent atmospheric noise $u(t)$, and the more narrow systems noise distribution $n(t)$ at a right angle. If we neglect for a moment the systems noise, we are left with atmospheric noise and a wanted signal amplitude.

Both atmospheric noise and wanted signal have a spatial coherence. This is represented by the auto-correlation in a certain direction in space. When the raw data is bandpass filtered, the correlation C_{jk} is expressed by:

$$C_{jk} = \frac{\sum_{t=1}^{T} (s_j(t) - \bar{s}_j)(s_k(t) - \bar{s}_k)}{[\sum_{t=1}^{T} (s_j(t) - \bar{s}_j)^2]^{1/2} [\sum_{t=1}^{T} (s_k(t) - \bar{s}_k)^2]^{1/2}} \qquad (27)$$

Where s_j and s_k are the sample values for the sensors j and k. $\bar{s}_j$ and $\bar{s}_k$ are the mean values of T samples. The expression is often referred to as normalized cross-correlation. Proper functioning of the array with low amplitude signals will depend on the short noise coherence length and a long signal coherence length. Coherence length is defined as the width of the auto-correlation as a function of distance between the stations. From the measurement it became clear that for noise a coherence length of smaller than 2 metre is typical for quiet weather. The signal coherence length exceeds 1000 metres for the frequencyband of 2-5 Hz.

Examples of array detections

From the Winter of 1991 onwards an acoustic array was operated at De Bilt. From the Summer of 1994 a second but smaller array was operated at Witteveen in the northern part of the Netherlands. The arrays registered a few events per day. Often the detections of the arrays are hard to trace back to certain events, nevertheless, we detected a large number of sonic booms. These dectections were from military airplanes and from the France and Brittish Concorde. In certain cases a thunderstorm was detected. The various thunderclaps made it possible to follow the trajectory of the storm. In many cases a number of reflections were recorded especially when the signals originated from the Concorde at distances larger than 1000 km.

Conclusions

In the development of the acoustic infrasonic array we borrowed the technique from seismograph arrays and used perhaps forgotten ideas with respect to the infrasonic detector. In this sense there is nothing new presented here. The purpose of this paper was to show how a low cost acoustic array can be operated with a minimum of effort with respect to data acquisition. By changing the sensors or the dimension of the array a wide variety of physical wave propagation phenomena can be investigated using this technique.

References

Backus, G. E., and J. F. Gilbert, The resolving power of gross earth data, *Geophys. J. Roy. Astron. Soc.*, **16**, 169-205, 1968.

Båth, M., Spectral analysis in Geophysics. *Elsevier*, 1974.

Battis, J. C., Temporal Attributes of the ambient Seismo-Acoustic Environment: La Junta Colorado, Air Force Geophysics Laboratory, AFGL-TR-89-0080, 1989.

Baumeler, Hp., Der Akustische Peiler, Gruppe Für Rüstungsdienste, Fachsektion Nachrichtentechniek, Reg. 2510/161/BAH, Bern, 15 August 1991.

Benioff, H., and B. Gutenberg, 1939. Waves and Currents Recorded by Electromagnetic Barographs, *Bull. of the Am. Meteor. Soc.*, **20**, 421-426, 1939.

Cansi, Y., J. L. Plantet, and B. Massinon, Earthquake location applied to a mini-array: k-spectrum versus correlation method, *Geophys. Res. Lett.*, **20**, 1819-1822, 1993.

Cook, R. K., and A. J. Bedard Jr., On the measurements of Infra Sound, *Geophys. J. Roy. Astron. Soc.*, **26**, 5-11, 1971.

Gold, T., and S. Soter, Brontides: Natural Explosive Noises, *Science*, **24**, 371-375, 1979.

Grachev, A. I., S. V. Zagoruyko, A. K. Matveyvev, and M. I. Mordukhovich, Some Findings on the Recording of Atmospheric Infrasonic Waves, *Izvestiya, Atmospheric and Oceanic Physics*, **14**, 340-345, 1978.

Gutenberg, B., The velocity of Sound Waves and the Temperature in the Stratosphere in Southern California, *Bull. Am. Meteor.Soc.*, **20**, 192-201, 1939.

Harjes, H.-P., Design and Siting of a New Regional array in Central Europe, *Bull. Seism. Soc. Am.*, **80**, 1801-1817, 1990.

Haubrich, R. A., Array Design, Bull. Seism. Soc. Am., **58**, 977-991, 1968.

Högbom, J. A., Aperture synthesis with a non regular distribution of interferometer baselines, *Astron. Astrophys. Suppl.*, **15**, 417-426, 1974.

Lee, W. H. K., Toolbox for Seismic Data Acquisition Processing, and Analysis, *IASPEI Software Library*, Volume I, 1989.

Nolet, G., and G. F. Panza, Array analysis of seismic surface waves, limits and possibilities. *Pure Appl. Geoph.*, **114**, 775-790, 1976.

Smart, E., and E. A. Flinn, Fast Frequency Wavenumber Analysis and Fisher Signal Detection in Real time Infrasonic Array Data Processing, *Geophys. J. Roy. Astr. Soc.*, **26**, 279-284, 1971.

Willmore, P. L., The application of the Maxwell Impedance bridge to the Calibration of Electromagnetic Seismographs, *Bull. Seism. Soc. Am.*, **49**, 99-114, 1959.

List of Figures

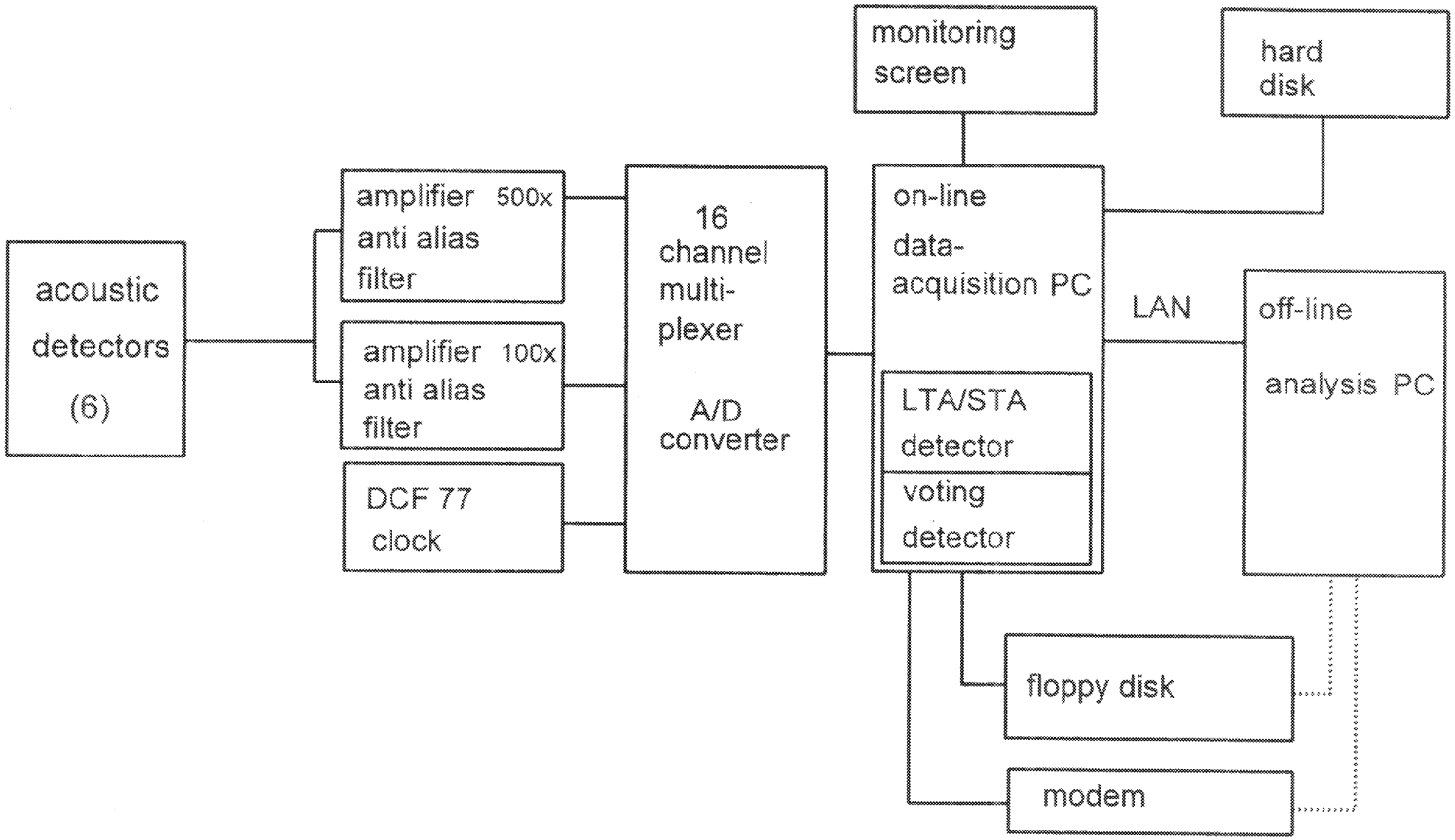

Figure 1. *Functional diagram of the PC-based acoustical array.*

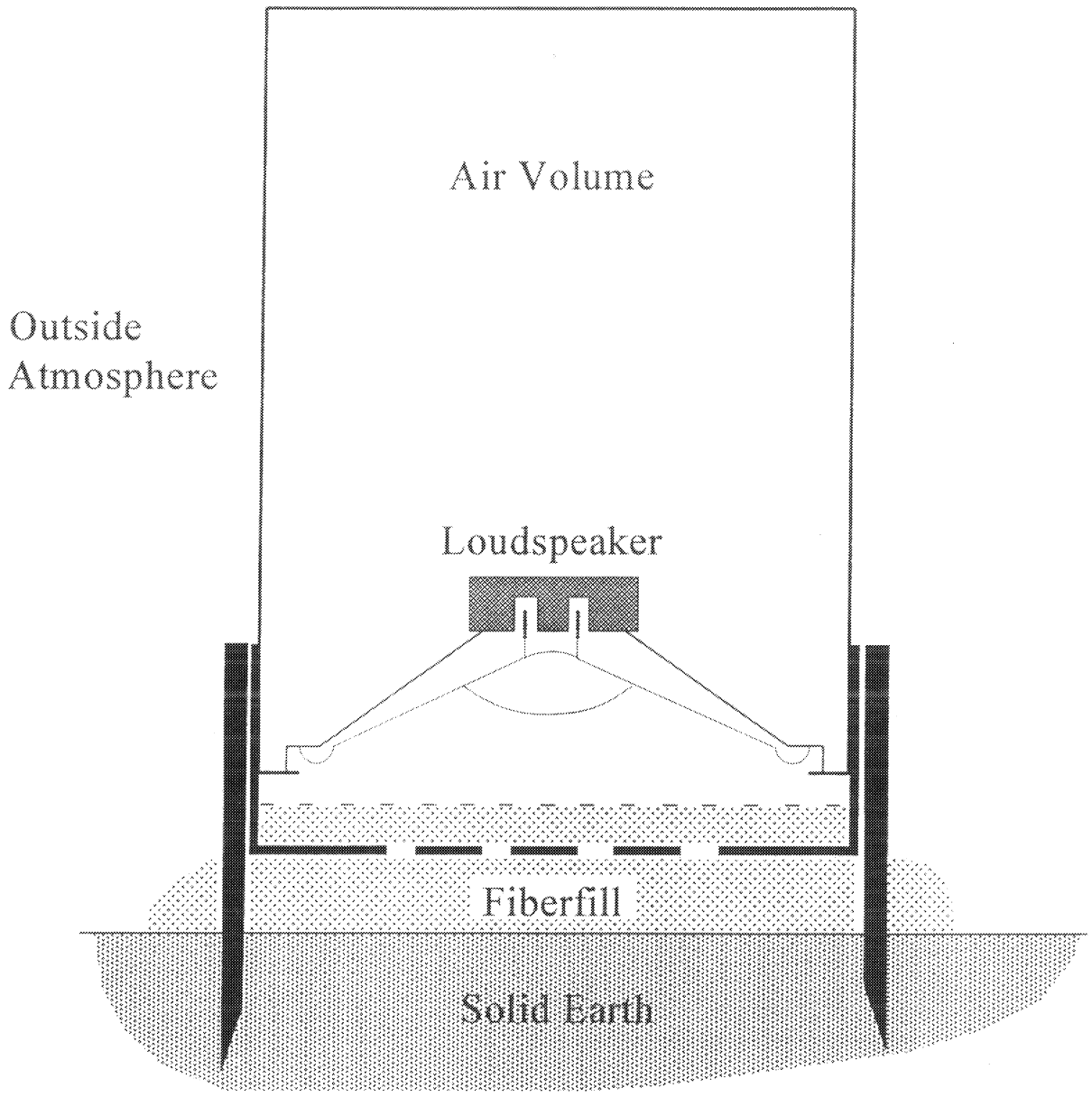

Figure 2. *Cross section of the low frequency acoustic detector.*

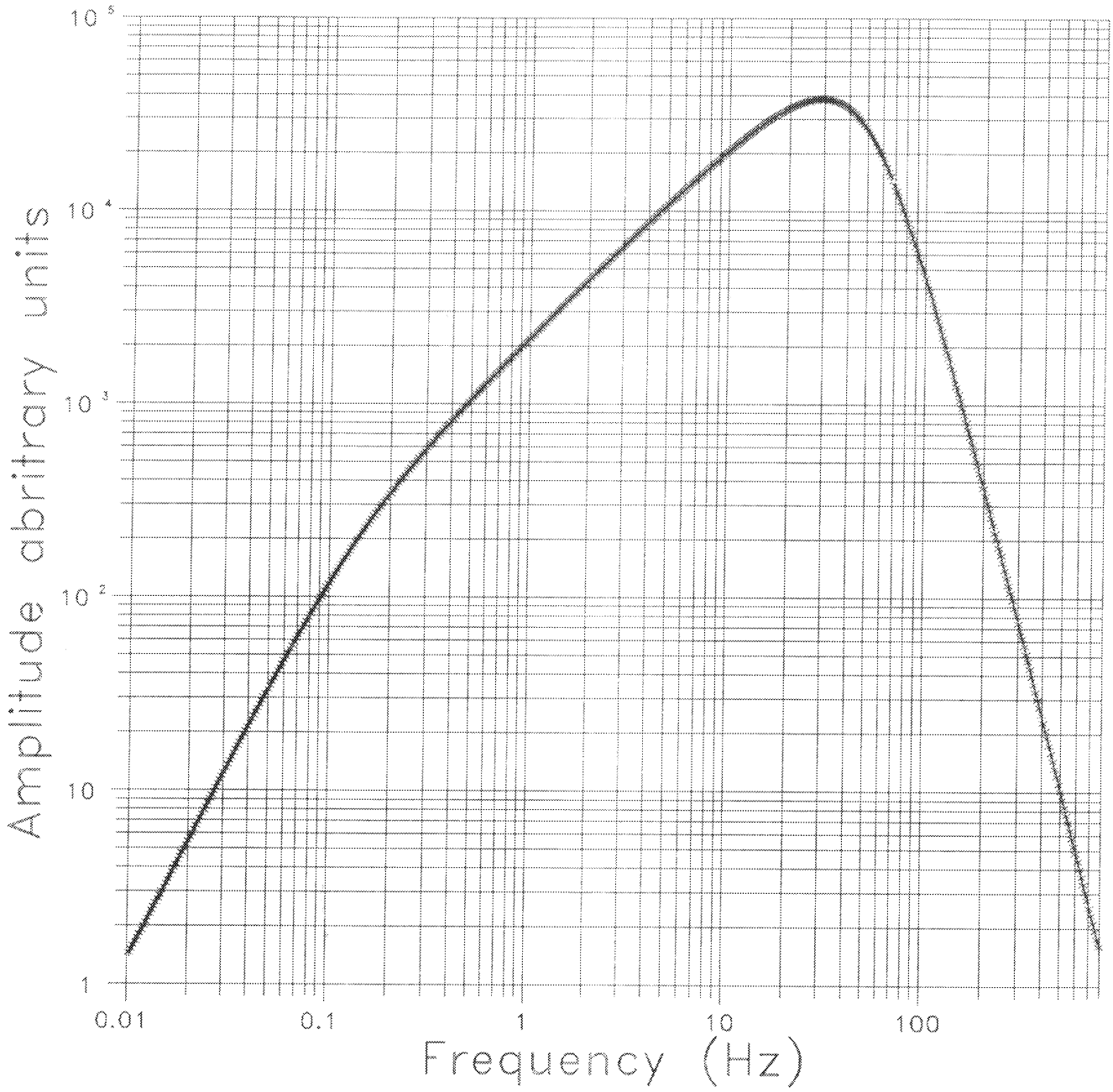

Figure 3. *Response of the acoustic detector.*

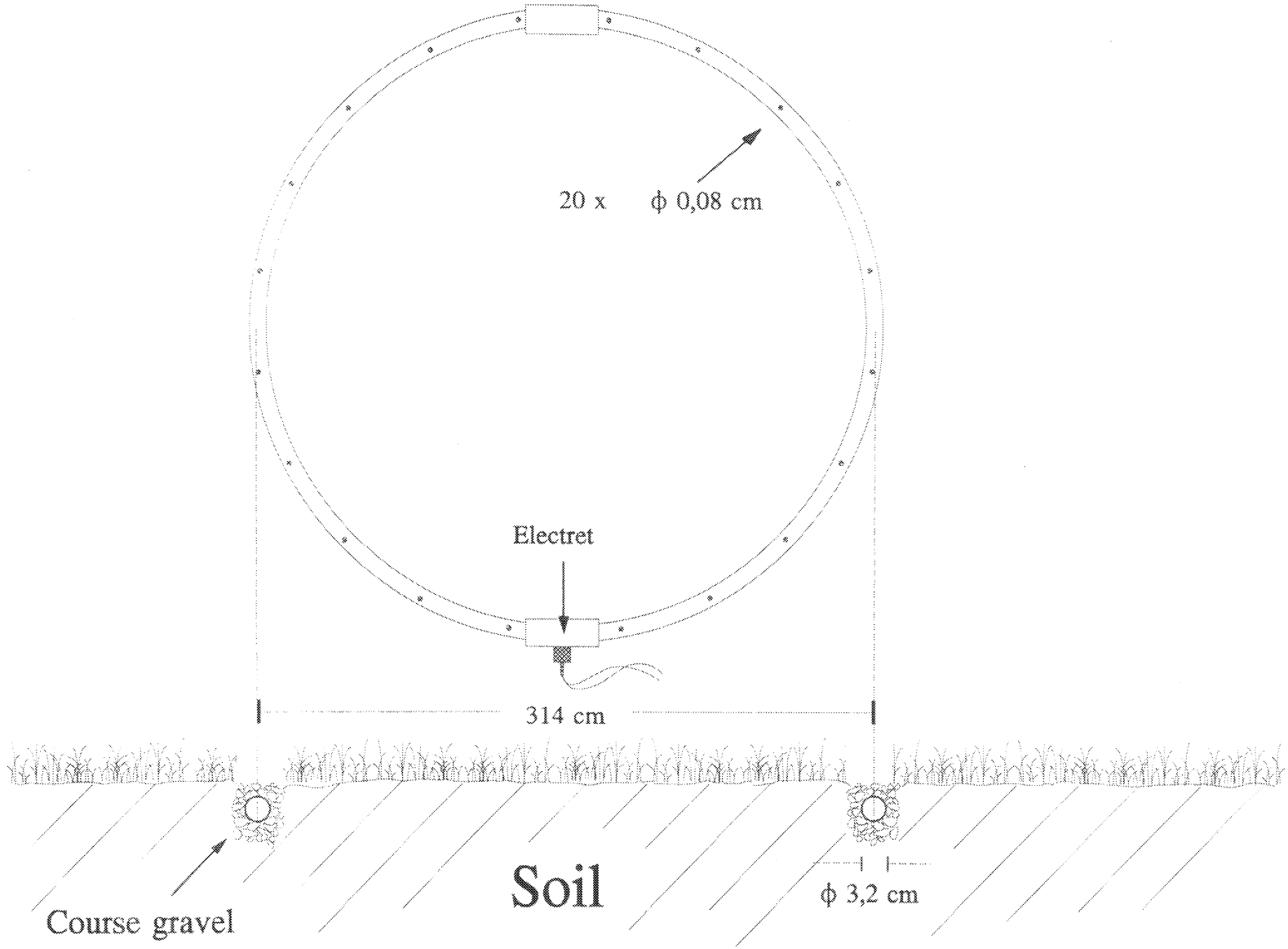

Figure 4. *Noise reducing structure with electret detector.*

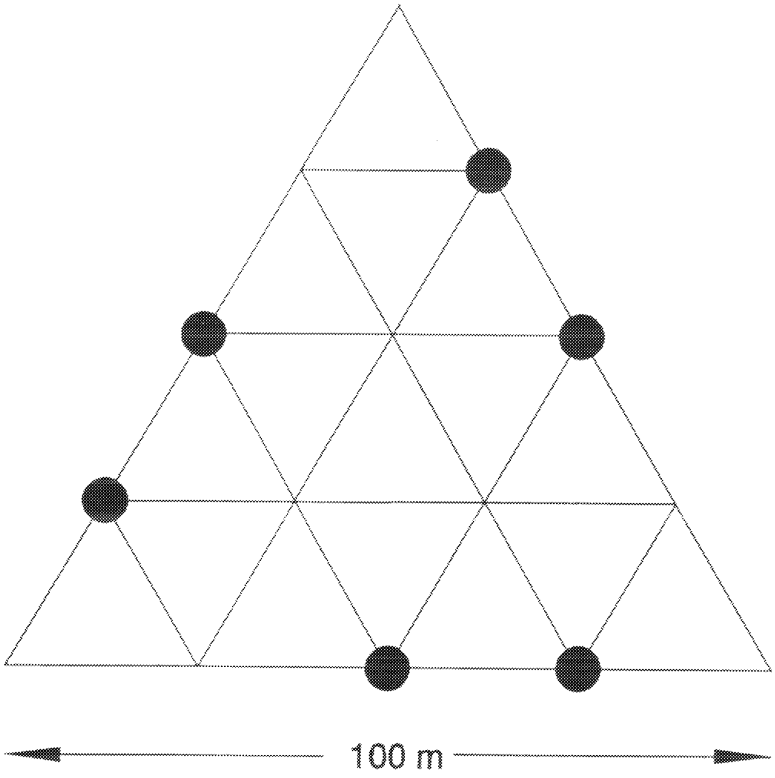

Figure 5a. *Lay-out of the six elements array.*

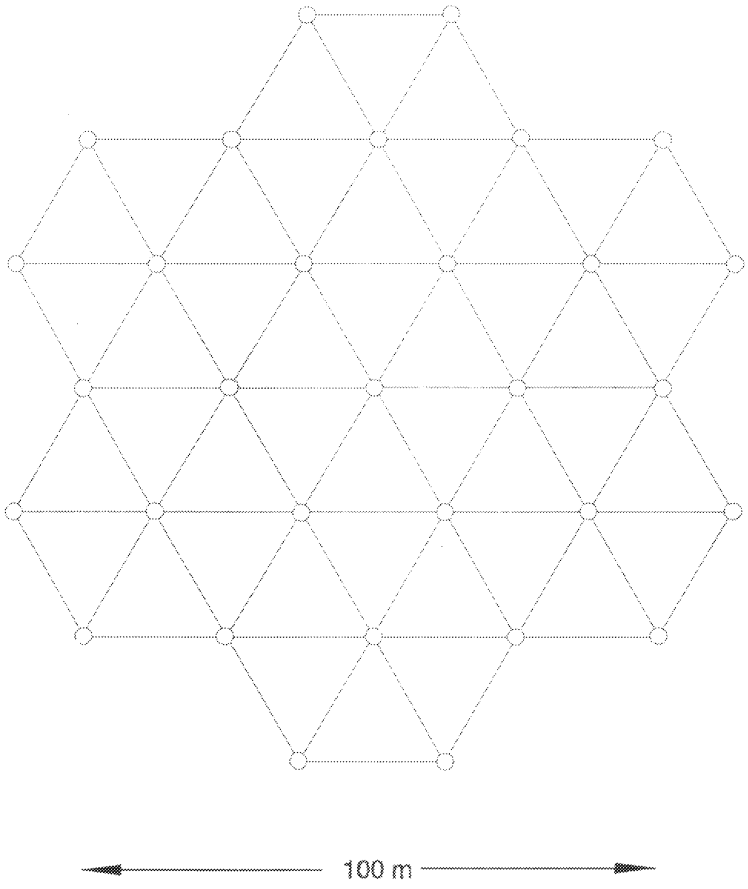

Figure 5b. *Coarray plot of the six elements array.*

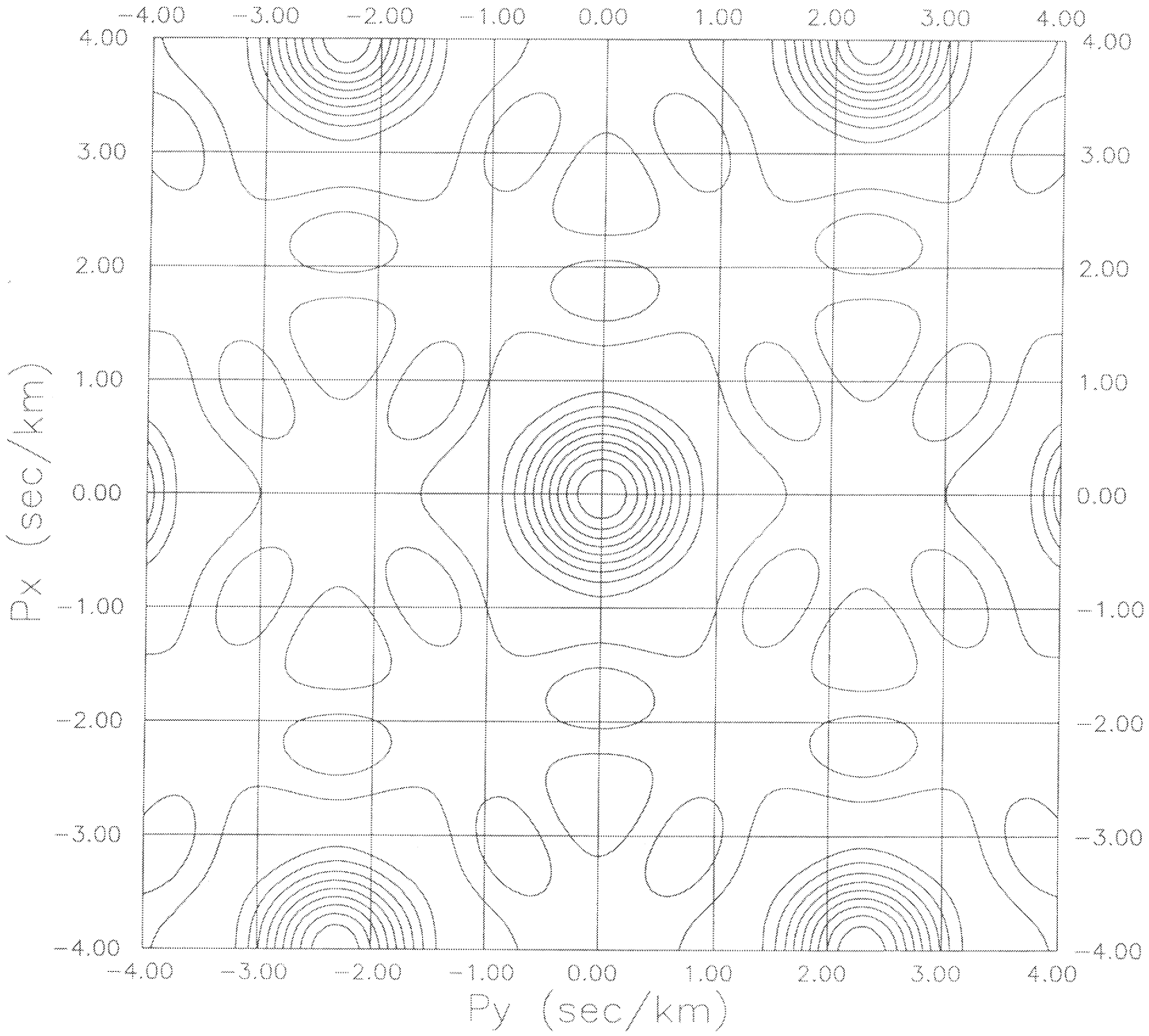

Figure 5c. *Array response: amplitude vs slowness at 10 Hz.*

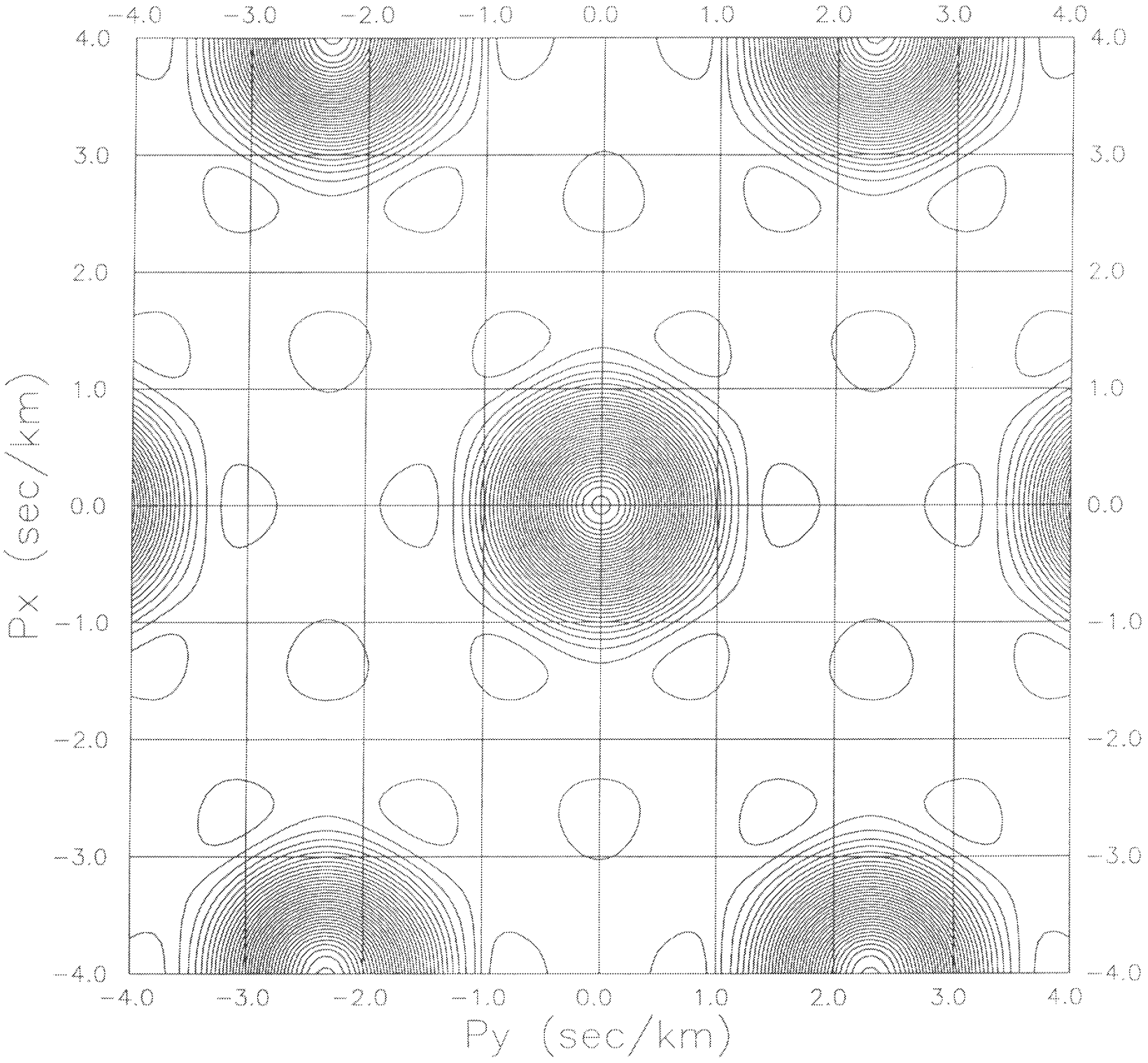

Figure 5d. *Array response: Hamming tapered amplitude vs slowness at 10 Hz.*

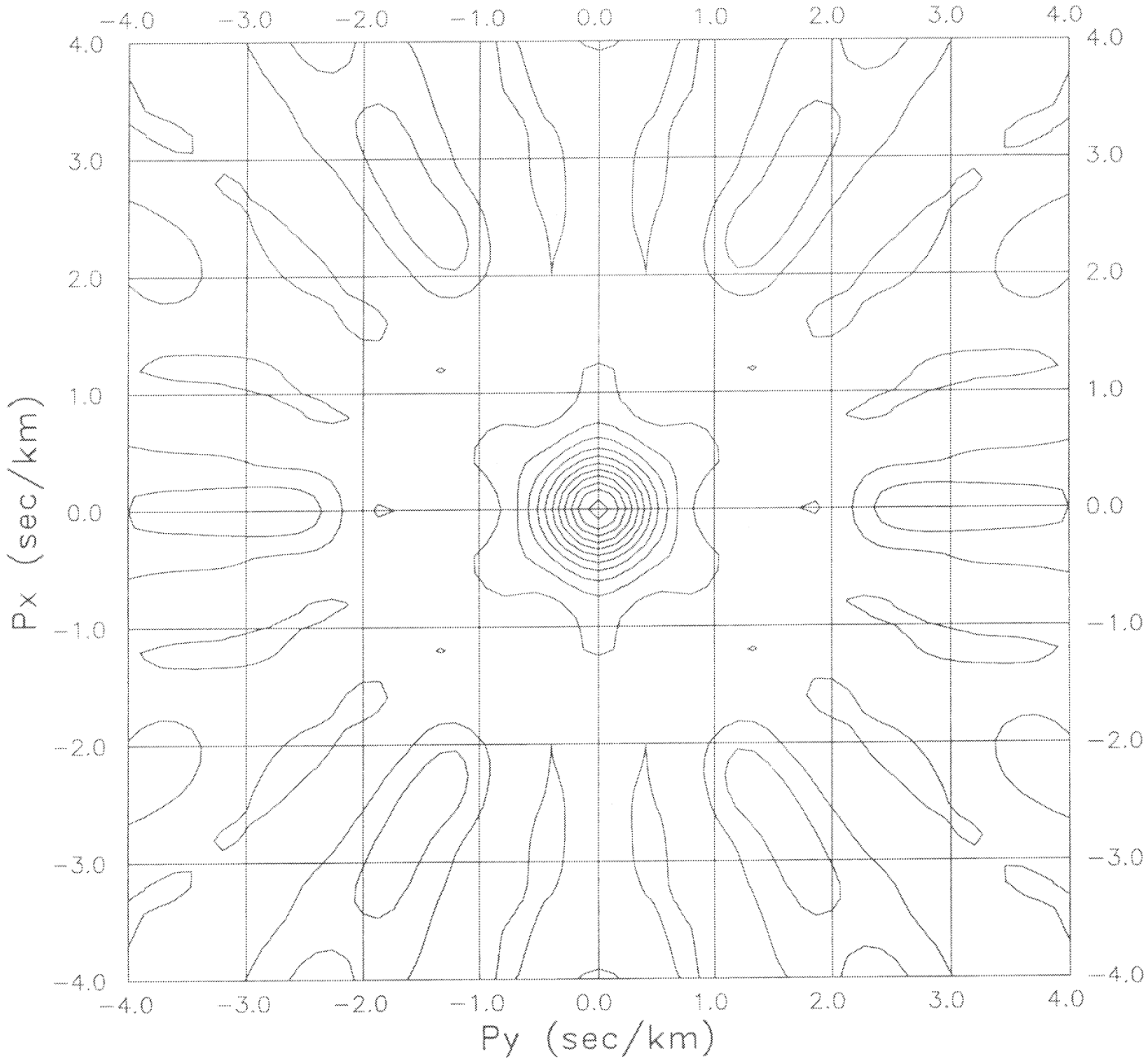

Figure 5e. *Array response: amplitude vs slowness over the bandwidth 5-20 Hz.*

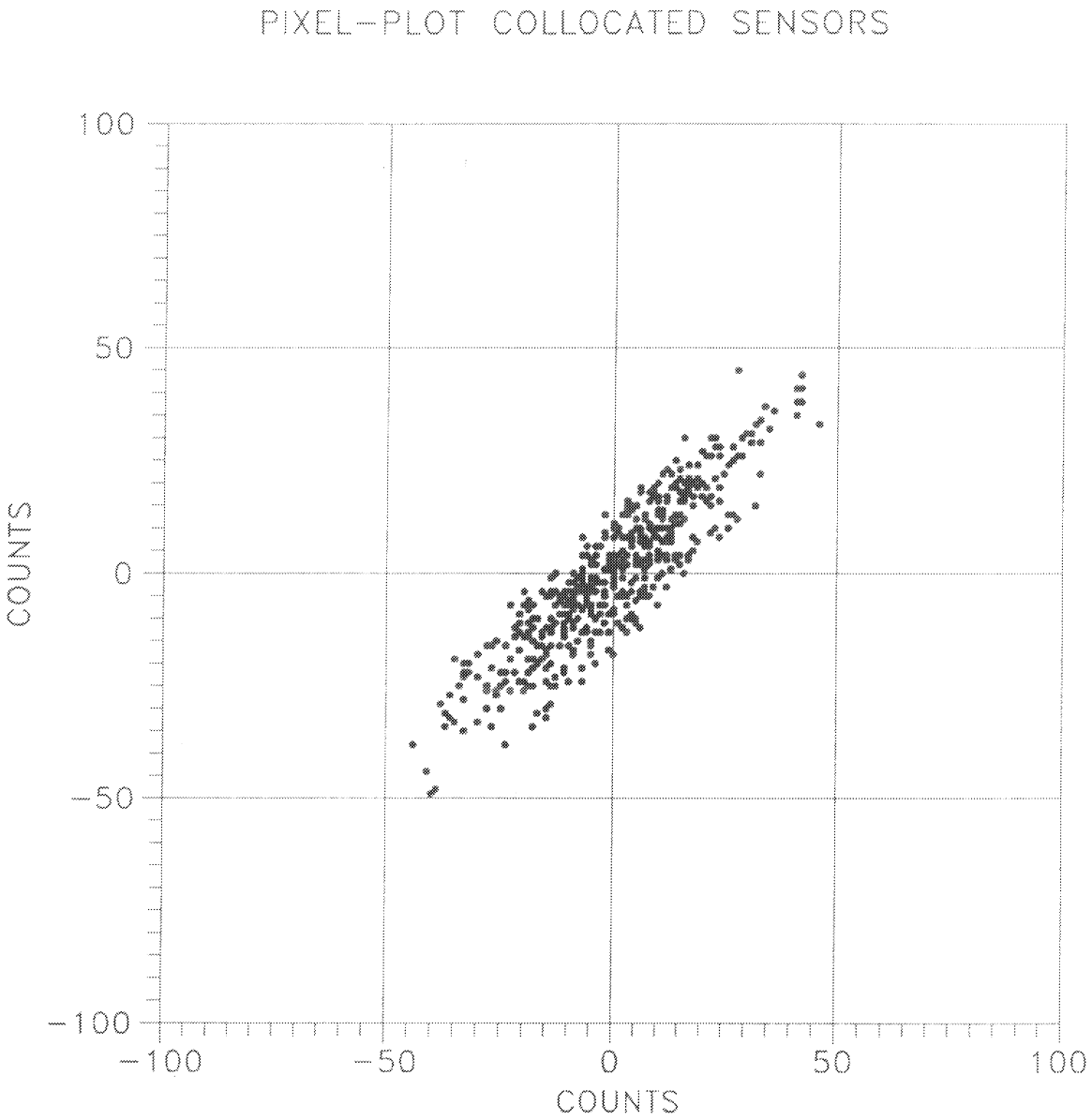

Figure 6. *Coherency plot.*

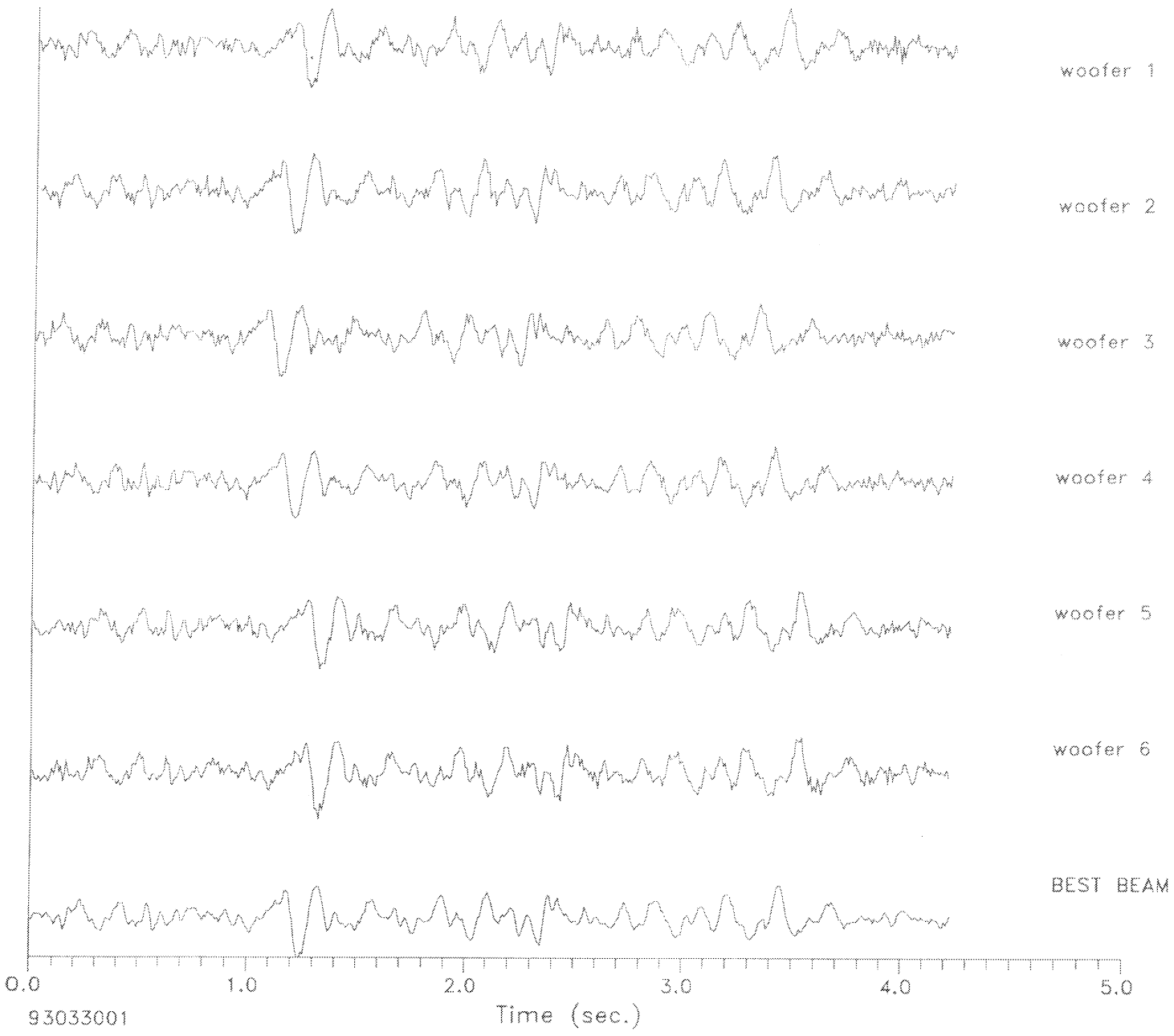

Figure 7. *Data example.*

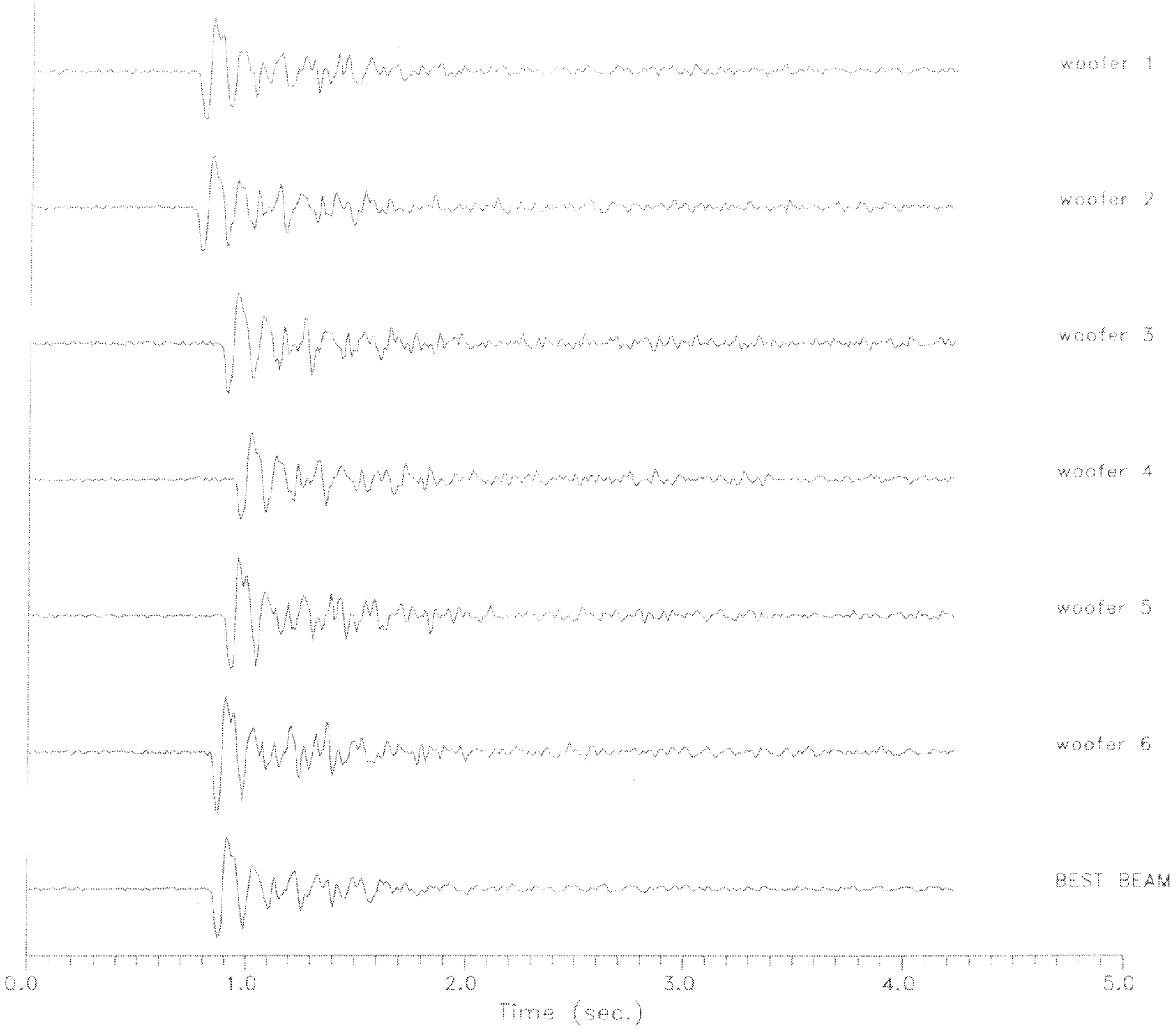

Figure 7. *Data example of the acoustic array.*

KNMI-Publicaties, Technische & Wetenschappelijke Rapporten gepubliceerd sedert 1988

Een overzicht van alle publicaties van het Koninklijk Nederlands Meteorologisch Instituut die tussen 1849 en 1988 werden uitgegeven, wordt u op verzoek toegezonden door de Bibliotheek van het KNMI, postbus 201, 3730 AE De Bilt, tel. 030 - 2 206 855, fax. 030 - 2 210 407.

KNMI-publicatie met nummer

150-27	Normalen en extreme waarden van 15 hoofdstations voor het tijdvak 1961-90 / samenst. H.J. Krijnen ...[et al.]	1992
165-5	Historische weerkundige waarnemingen: beschrijving antieke meetreeksen / H.A.M. Geurts en A.F.V. van Engelen	1992
172	Vliegen in weer en wind: geschiedenis van de luchtvaartmeteorologie / Tj. Langerveld	1988
173	Werkdocument verspreidingsmodellen / red. H. van Dop ; in samenwerking met het RIVM	1988
174	Ons klimaat, onze planeet / voorw. H. Tennekes ; inleiding C.J.E. Schuurmans ; met bijdr. van H. van Dop ...[et al.]	1989
175	Klimaat-onderzoek Westland ten behoeve van kustuitbreiding / W.H. Slob	1989
176	Stormenkalender: chronologisch overzicht van alle stormen langs de Nederlandse kust 1964-1990 / B. Augustijn, H. Daan ...[et al.]	1990
177	Description of the RIVM-KNMI PUFF dispersion model / G.H.L. Verver ...[et al.]	1990
178	Modules A & B / Bureau Vorming en Opleiding **[uitsluitend intern beschikbaar]**	1991-
179	Catalogus van aardbevingen in Nederland / G. Hougast	1991
179a	Catalogus van aardbevingen in Nederland : 2e, gewijzigde druk / G. Houtgast	1992
180	List of acronyms in environmental sciences / [P. Geerders]	1991
180a	List of acronyms in environmental sciences : revised edition / [P. Geerders and M. Waterborg]	1995
181	Nationaal gebruik van de groepen 7wwW1W2 en 960ww voor landstations / [samenst. H. van Drongelen ea.]	1992
181a	FM12 Synop : internationale en nationale regelgeving voor het coderen van de groepen 7wwW1W2 en 960ww	1995
182	Wijziging aeronautische codes : 1 juli 1993 / [P.Y. de Vries en A.A. Brouwer]	1993
183-1	Rainfall in New Guinea (Irian Jaya) / T.B. Ridder	1995
183-2	Vergelijking van zware regens te Hollandia (Nieuw Guinea), thans Jayapura (Irian Jaya) met zware regens te De Bilt / T.B. Ridder	1995
183-3	Verdamping in Nieuw-Guinea, vergelijking van gemeten hoeveelheden met berekende hoeveelheden / T.B. Ridder	1995
183-4	Beschrijving van het klimaat te Merauke, Nieuw Guinea (Irian Jaya) in verband met de eventuele vestiging van een zoutwinningsbedrijf aldaar / T.B. Ridder en H.W.H. Weeda	1995
183-5	Overzicht van klimatologische en geofysische publikaties betreffende Nieuw-Guinea / T.B. Ridder	1995
184	Inleiding tot de algemene meteorologie : studie-uitgave / B. Zwart, A. Steenhuisen, m.m.v. H.J. Krijnen	1994
184a	Inleiding tot de algemene meteorologie : studie uitgave ; 2e, geheel herziene druk / B. Zwart, A. Steenhuisen, m.m.v. H.J. Krijnen ea.	1995
185	Handleiding voor het gebruik van sectie 2 van de FM 13-X SHIP code door stations op zee / KNMI; Kon. Luchtmacht; Kon. Marine	1994
185a	Handleiding voor het gebruik van sectie 2 van de FM 13-X SHIP-code voor waarnemers op zee / KNMI; Kon.Luchtmacht, Kon.Marine	1995
(-)	Zonnestraling in Nederland / C.A. Velds (i.s.m. uitgeverij Thieme in de serie Het klimaat van Nederland; 3)	1992

Technisch rapport = technical report (TR) - ISSN 0169-1708

103a	Wind-chill [geheel herziene versie] / B. Zwart	1992
105	Description of the Cabauw turbulence dataset 1977-1979 / C. Hofman	1988
106	Automatische detektie van inversies met sodar / A.C.M. Beljaars en R. Agterberg	1988
107	Numerieke atmosfeermodellen / A.P.M. Baede	1988
108	Inpassing van Meteosat informatie in de meteorologische besluitvorming / J. Roodenburg	1988
109	Opmeting van het aardmagneetveld in Nederland, herleid naar 1985 / J.H. Rietman	1988
111	Van Penman naar Makkink: een nieuwe berekeningswijze voor de klimatologische verdampingsgetallen / red. J.C. Hooghart ...[et al.]	1988
112	Description of a software library for the calculation of surface fluxes / A.C.M. Beljaars ...[et al.]	1989
113	Menghoogteberekeningen voor het Europees continent: een vergelijkend onderzoek / M.P. Scheele en H. van Dop	1989
114	Operational WAMS statistics over the period December 1986 - March 1987 / R.A. van Moerkerken ...[et al.]	1989
115	Mesoscale terrain roughness mapping of the Netherlands / R. Agterberg and J. Wieringa	1989
116	Geschiedenis van de landbouwmeteorologie in Nederland tot 1972 / J.P.M. Woudenberg	1989
117	Instabiliteiten rond de straalstroom / R.P. Henzen	1989
118	Verfificatie van de GONO golfverwachting over de periode oktober 1987 - april 1988 / R.A. van Moerkerken	1989
119	Spectra en gradienten van hoge windsnelheden te Cabauw tot 200 meter / R.W.M. Meijer	1989
120	About the possibilities of using an air transformation model in Tayun, Shanxi province, China / J. Reiff ...[et al.]	1989
121	The effect of wave data assimilation of the numerical simulation of wave energy advection / M. de las Heras ...[et al.]	1990
122	Objective analysis of precipitation observations during the Chernobyl episode / M.P. Scheele and G.H. Verver	1990
123	The use of satellite data in the ECMWF analysis system / K. Lablancz	1990
124	A primitive equation model for the Equatorial Pacific / M.A.F. Allaart and A. Kattenberg	1990
125	Technical description of the high-resolution air mass transformation model at KNMI / E.I.F. de Bruin ...[et al.]	1990
126	Verificatie kwantitatieve neerslagverwachting korte termijn (proefperiode) voor 5 regio's / D. Messerschmidt	1990
127	Quantitative processing of Meteosat-data: implementation at KNMI: applications / S.H. Muller	1990
128	A primary experiment of statistical interpolation schemes used in sea wave data assimilation / Gao Quanduo	1990
129	Coordinate conversions for presenting and compositing weather radar data / H.R.A. Wessels	1990
130	Flux-profile relationships in the nocturnal boundary layer / P. Bouwman	1990
131	The implementation of the WAQUA/CSM-16 model for real time storm surge forecasting / J.W. de Vries	1991
132	De luchttemperatuur boven West-Ameland / F. Ynsen	1991
133	Seizoenverloop en trend in de chemische samenstelling van de neerslag te Lelystad / T.A. Buishand en J.H. Baard	1991
134	Technical description of LAM and OI: Limited Area Model and Optimum Interpolation analysis / W.C. de Rooy ...[et al.]	1991
134a	Technical description of LAM and OI: Limited Area Model and Optimum Interpolation analysis, 2nd edition / W.C. de Rooy ...[et al.]	1992
135	Relatieve trajectorien in en rond een depressie / J.P.A.J. van Beeck	1991
136	Bepaling van een directe en diffuse straling en van zonneschijnduur uit 10-minuutwaarden van de globale straling / W.H. Slob ...[et al.]	1991
137	LAM en NEDWAM statistics over the period October 1990 - April 1991 / R.A. van Moerkerken	1991
138	Dagsom van de globale straling : een rekenmethode en verwachtingsverificatie / M.C. Nolet	1991
139	A real-time wave data quality control algorithm / Maria Paula Etala	1991
140	Syllabus Fysische Meteorologie I / H.R.A. Wessels	1991
141	Systeembeschrijving Mist Voorspel Systeem MIVOS / D. Blaauboer, H.R.A. Wessels en S. Kruizinga	1992
142	Het nachtelijk windmaximum : een interactieve verwachtingsmethode / N. Maat en H. Bakker	1992
143	Neerslagverificatie LAM / W.C. de Rooy en C. Engeldal	1992
144	Aanpassing vocht-bedekkingsgraadrelaties in het LAM / W.C. de Rooy	1992
145	Een verificatie van de Eurogids, de gidsverwachting voor vervoer en toerisme / H.G. Theihzen	1992

146 The earth radiation budget experiment : overview of data-processing and error sources / Arnout J. Feijt 1992
147 On the construction of a regional atmospheric climate model / Jens H. Christensen and Erik van Meijgaard 1992
148 Analyse van torenwindgegevens over het tijdvak 1977 tot en met 1991 / Gertie Geertsema 1992
149 The performance of drag relations in the WAQUA storm surge model / J.R.N. Onvlee 1993
150 Verifications of 3I retrievals vis-à-vis radiosonde observations / G.J. Prangsma 1993
151 Het Synoptisch Symposium : een verslag / red. H.G. Theihzen 1993
152 The ACIFORN hydrological programme : the water cycle of a Douglas fir forest / F.C. Bosveld ...[et al.] 1993
153 Het APL+-prgramma / R.M. van Westrhenen 1993
154 The effect of spatial averaing on threshold exceedances of daily precipitation amounts / T.A. Buishand, 1993
155 Neerslagvergelijking van Espelo ten opzichte van het omgevingsgemiddelde / J.P.M. van Dun en J. Verloop 1993
156 On the effects of limited spectral resolution in third-generation wave models / I.V. Lavrenov and J.R.A. Onvlee 1993
157 Meteorologische evaluatie van de zichtmetingen langs de A16 / H.R.A. Wessels 1993
158 Het programma voor berekening van zonneschijnduur uit globale straling / U. Bergman 1993
159 Verificatie weersverwachtingen 1955 - 1993 / H. Daan 1993
160 Drie objectieve indices voor clear-air turbulence nader bekeken / H. Bakker 1993
161 The ASGASEX experiment / W.A. Oost 1994
162 TEBEX observations of clouds and radiation -potential and limitations / P. Stammes ...[et al.] 1994
163 Evaluatie kwaliteitsonderzoek mistdata "Mistprojekt A-16" Breda / M. van Berchum 1994
164 Standaard stralingsmetingen met een zonnevolger / A.C.A.P. van Lammeren en A. Hulshof 1994
165 Neurale netwerken versus lineaire regressie / R.M. Meuleman 1994
166 Seismische analyse van de aardbeving bij Alkmaar op 6 augustus 1994 / [SO] 1994
167 Seismische analyse van de aardbeving bij Alkmaar op 21 september 1994 / [SO] 1994
168 Analyse van het seismische risico in Noord-Nederland / Th. de Crook, B. Dost en H.W. Haak 1995
169 Evaluatie van neerslagprognoses van numerieke modellen voor de Belgische Ardennen in december 1993 / Erik van Meijgaard 1994
170 DARR-94 / C.P.G. Lomme 1994
171 EFEDA-91 : documentation of measurements obtained by KNMI / W.A.A. Monna ...[et al.] 1994
172 Cloud lidar research at the Royal Netherlands Meteorological Institute and KNMI2B2 version 2 cloud lidar analysis software documentation / Alexandre Y. Fong and André C.A.P. van Lammeren 1994
173 Measurements of the structure parameter of vertical wind-velocity in the atmospheric boundary layer / R. van der Ploeg 1995
174 Report of the ASGASEX'94 workshop / ed. by W.A. Oost 1995
175 Over slecht zicht, bewolking, windstoten en gladheid / J. Terpstra 1995
176 Verification of the WAQUA/CSM-16 model for the winters 1992-93 and 1993-94 / J.W. de Vries 1995
177 Nauwkeuriger nettostraling meten / M.K. van der Molen en W. Kohsiek 1995
178 Neerslag in het stroomgebied van de Maas in januari 1995: waarnemingen en verificatie van modelprognoses / Rudmer Jilderda ...[et al.] 1995
179 First field experience with 600PA phased array sodar / Henk Klein Baltink 1995
180 Een Kalman-correctieschema voor de wegdektemperatuurverwachtingen van het VAISALA-model / A. Jacobs 1995
181 Calibration study of the K-Gill propeller vane / Marcel Bottema 1995
182 Ontwikkeling van een spectraal UV-meetinstrument / Frank Helderman 1995
183 Rainfall generator for the Rhine catchment : a feasibility study / T. Adri Buishand and Theo Brandsma 1996
184 Parametrisatie van mooi-weer cumulus / M.C. van Zanten 1995
185 Interim report on the KNMI contributions to the second phase of the AERO-project / Wiel Wauben, Paul Fortuin ...[et al.] 1995
186 Seismische analyse van de aardbevingen bij Middelstum (30 juli 1994) en Annen (16 augustus 1994 en 31 januari 1995) / [SO] 1995
187 Analyse wenselijkheid overname RIVM-windmeetlokaties door KNMI / H. Benschop 1996
188 Windsnelheidsmetingen op zeestations en kuststations; herleiding waarden windsnelheden naar 10-meter niveau / H. Benschop 1996
189 On the KNMI calibration of net radiometers / W. Kohsiek 1996
190 NEDWAM statistics over the period October 1994 - April 1995 / F.B. Koek 1996
191 Description and verification of the HIRLAM trajectory model / E.I.F. de Bruijn 1996
192 Tiltmeting : een alternatief voor waterpassing ? / H.W. Haak 1996

Wetenschappelijk rapport = scientific report (WR) - ISSN 0169-1651

88-01 Central Sudan surface wind data and climate characteristics / E.H. ABu Bakr
88-02 Startocumulus modeling / P.G. Duynkerke
88-03 Naar een niet-linear wateropzetmodel : stand van zaken februari 1988 / C.J. Kok
88-04 The boundary layer wind regime of a representative tropical African region, central Sudan / E.H. ABu Bakr
88-05 Radiative cooling in the nocturnal boundary layer / S.A. Tjemkes
88-06 Surface flux parameterization schemes : developments and experiences at KNMI / A.A.M. Holtslag and A.C.M. Beljaars
89-01 Instability mechanisms in a barotropic atmsophere / R.J. Haarsma
89-02 Climatological data for the North Sea based on observations by volutary observing ships over the period 1961-1980 / C.G. Korevaar
89-03 Verificatie van GONO golfverwachtingen en van Engelse fine-mesh winden over de periode oktober 1986 - april 1987 / R.A. van Moerkerken
89-04 Diagnostics derivation of boundary layer parameters from the outputs of atmospheric models / A.A.M. Holtslag ...[et al.]
89-05 Statistical forecasts of sushine duration / Li Zhihong and S. Kruizinga
90-01 The effect of a doubling atmospheric CO2 on the stormtracks in the climate of a GCM / P.C. Siegmund
90-02 Analysis of regional differences of forecasts with the multi-layer AMT-model in the Netherlands / E.I.F. de Bruin, Li Tao Guang ...[et al.]
90-03 Description of the CRAU- data-set: Meteosat data, radiosonde data, sea surface temperatures : comparison of Meteosat and Heimann-data / S.H. Muller, H. The, W. Kohsiek and W.A.A. Monna
90-04 A guide to the NEDWAM wave model / G. Burgers
91-01 A parametrization of the convective atmospheric boundary layer and its application into a global climate model / A.A.M. Holtslag ...[et al.]
91-02 Turbulent exchange coefficients over a Douglas fir forest / F.C. Bosveld
92-01 Experimental evaluation of an arrival time difference lightning positioning system / H.R.A. Wessels
92-02 GCM control run of UK Met.Office compared with the real climate in the Northwest European winter / J.J. Beersma
92-03 The parameterization of vertical turbulent mixing processes in a General Circulation Model of the Tropical Pacific / G. Janssen
92-04 A scintilation experiment over a forest / W. Kohsiek
92-05 Grondtemperaturen / P.C.T. van der Hoeven en W.N. Lablans
92-06 Automatic supression of anomalous propagation clutter for noncoherent weather radars / H.R.A. Wessels ...[et al.]
93-01 Searching for stationary stable solutions of Euler's equation / R. Salden
93-02 Modelling daily precipitation as a function of temperature for climatic change impact studies / A.M.G. Klein Tank and T.A. Buishand
93-03 An analytical conceptual model of extratropical cyclones / L.C. Heijboer

93-04 A synoptic climatology of convective weather in the Netherlands / Dong Hongnian
93-05 Conceptual models of severe convective weather in the Netherlands / Dong Hongnian
94-01 Seismische analyse van aardbevingen in Noord-Nederland : bijdrage aan het multidisciplinaire onderzoek naar de relatie tussen gaswinning en aardbevingen / H.W. Haak en Th. de Crook
94-02 Storm activity over the North Sea and the Netherlands in two climate models compared with observations / J.J. Beersma
94-03 Atmospheric effects of high-flying subsonic aircraft / W. Fransen
94-04 Cloud-radiation-hydrological interactions : measuring and modeling / A. Feijt ...[et al.]
94-05 Spectral ultraviolet radiation measurements and correlation with atmospheric parameters / F. Kuik and H. Kelder
95-01 Transformation of precipitation time series for climate change impact studies / A.M.G. Klein Tank and T.A. Buishand
95-02 Internal variability of the ocean generated by a stochastic forcing / M.H.B. van Noordenburg
95-03 Applicability of weakly nonlinear theory for the planetary-scale flow / E.A. Kartashova
95-04 Changes in tropospheric NOx and O3 due to subsonic aircraft emissions / W.M.F. Wauben ...[et al.]
95-05 Numerical studies on the Lorenz-84 atmosphere model / Leonardo Anastassiades
95-06 Regionalisation of meteorological parameters / W.C. de Rooy
95-07 Validation of the surface parametrization of HIRLAM using surface-based measurements and remote sensing data / A.F. Moene, H.A.R. de Bruin ...[et al.]
95-08 Probabilities of climatic change : a pilot study / Wieger Fransen (ed.) and Alice Reuvekamp
96-01 A new algorithm for total ozone retrieval from direct sun measurements with a filter instrument / W.M.F. Wauben
96-02 Chaos and coupling: a coupled atmosphere ocean-boxmodel for coupled behaviour studies / G. Zondervan
96-03 An acoustical array for subsonic signals / H.W. Haak